THE JOURNAL OF PROSTHETIC DENTISTRY

CLINICAL RESEARCH

Assessment of distortion of intraoral scans of edentulous mandibular arch made with a 2-step scanning strategy: A clinical study

Lucio Lo Russo, DDS, PhD,[a] Roberto Sorrentino, DDS, PhD,[b] Fariba Esperouz, DDS,[c] Fernando Zarone, DDS,[d] Carlo Ercoli, DDS, MBA,[e] and Laura Guida, DDS[f]

ABSTRACT

Statement of problem. Manufacturers of several intraoral scanners have recommended a 2-step strategy for scanning the edentulous mandible. The 2-step technique requires scanning one side first and then moving to the other side. However, whether inconsistency in stitching occurs that results in loss of accuracy or distortion is unclear.

Purpose. The purpose of this clinical study was to measure the potential distortion of intraoral scans of edentulous mandibular arches made with a 2-step scanning strategy and to assess their differences with conventional impressions.

Material and methods. Twenty mandibular edentulous arches were scanned by 1 investigator with an intraoral scanner using a 2-step scanning strategy, and a corresponding polysulfide conventional impression was obtained. The conventional impression was then immediately scanned with the same intraoral scanner. The obtained standard tessellation language (STL) files were superimposed with a surface-matching software program. After a preliminary alignment, the STL meshes were trimmed and reoriented; then, the final alignment was carried out and meshes moved to a metrology software program where their mean distance was measured. In addition, a surface curve (SIOS) was traced on the intraoral scan from the right to left retromolar pad along the residual ridge and automatically projected onto to the conventional impression scan to obtain a new curve (SC). The mean distance between SIOS and SC was measured and recorded as an indicator of the distortion by considering the X-, Y-, and Z-axes and the overall 3-dimensional (3D) deviation. The analysis was performed for the full curve length and after dividing it into 6 regions of interest. Univariate and multivariate statistical analyses were used to investigate the significance of the extent of the mean 3D distance, as well as the effects of measurement positions (side and region) between and within patients on differences along the X-, Y-, and Z-axes (α=.05).

Results. The mean (−0.08 mm; standard error: 0.025) 3D distance between the intraoral scan and conventional impression was significantly different from zero (P=.003). No significant effect of the factor "side" was found by using generalized estimated equation models for the X-, Y-, and Z-axes, and global 3D deviations between SIOS and SC (P>.05), which appeared to exclude distortion. Conversely, a significant effect was found for the factor "region" (P<.05), with no significant differences (P>.05) between corresponding regions on the 2 sides.

Conclusions. Intraoral scans of the edentulous mandibular arch made in a 2-step procedure did not exhibit significant distortion in comparison with conventional impressions. (J Prosthet Dent xxxx;xxx:xxx-xxx)

This research did not receive any specific grant from funding agencies in the public, commercial, or not-for-profit sectors.
The authors declare the following financial interests/personal relationships which may be considered as potential competing interests: Prof Lo Russo has stock ownership in ELDO srl, the manufacturer of retractors used in the study.

[a]Professor of Prosthodontics, Department of Clinical and Experimental Medicine, School of Dentistry, University of Foggia, Foggia, Italy.
[b]Professor of Prosthodontics, Department of Neurosciences, Reproductive and Odontostomatological Sciences, Scientific Unit of Digital Dentistry, University "Federico II" of Naples, Naples, Italy.
[c]Resident, Department of Clinical and Experimental Medicine, School of Dentistry, University of Foggia, Foggia, Italy.
[d]Professor of Prosthodontics, Department of Neurosciences, Reproductive and Odontostomatological Sciences, Scientific Unit of Digital Dentistry, University "Federico II" of Naples, Naples, Italy.
[e]Professor, Prosthodontics and Periodontics, Chair, Department of Prosthodontics, Eastman Institute for Oral Health, University of Rochester, Rochester, NY.
[f]Private practice, Vallesaccarda, Italy.

Clinical Implications

The recommendation of intraoral scanner manufacturers of a 2-step scanning strategy for the edentulous mandible should yield accurate scans when combined with adequate residual ridge tissue management.

Intraoral scans of edentulous arches have been successfully used in the fabrication of removable dental prostheses[1,2] and offer clinical and practical advantages[3] for the patient and dental practices. Although the accuracy of intraoral scans of edentulous arches has been demonstrated in clinical studies,[4,5] debate still exists in regard to their suitability for clinical use.[6] This criticism, mainly rooted in the observation that differences with conventional impressions exist, is, however, clouded with methodological issues related to the mucostatic or mucocompressive nature of the resultant recordings, which have yet to be adequately addressed. The accuracy of intraoral scans has been determined from an in vitro study[7] to be comparable with that of conventional impressions, although considerable variability has been highlighted.[8]

Strategies to improve the accuracy of edentulous arch intraoral scans and/or facilitate image capturing have been proposed, including the application of artificial landmarks,[9,10] in an attempt to address the lack of anatomic variation and reference points in edentulous arches, which might introduce errors in the images-stitching process.[11] While these strategies have been published,[9,10] their usefulness is yet to be adequately demonstrated. Indeed, the absence of teeth or other fixed landmarks does not necessarily imply the absence of scannable geometric features because the macroscopic geometry and texture of the edentulous ridge mucosa has few, if any, differences compared with the gingiva.[12] Thus, the greatest difference between gingiva and mucosa is not the absence of scannable geometric landmarks but the instability of the mucosal tissues. With residual ridge resorption[13] after tooth loss and the consequent loss of the alveolar component of the edentulous arches, the residual ridge can be significantly reduced in volume, or its stability undermined by the presence of flabby tissues.[14] Hence, intraoral scanning of the edentulous arches may be challenging because the stitching process may be impaired by tissue instability, especially in the edentulous mandible. Therefore, to improve the feasibility and accuracy of the intraoral scanning of edentulous arches, the scanning field should ideally remain unaltered for the time required to complete the scanning procedure. This requirement is strictly correlated and acts in synergy with the scanning strategy: in a simplistic way, the scanning strategy, which has been demonstrated to affect the accuracy of intraoral scanning,[7] is a specific pattern and sequence of movements of the scanner above the scanning field. While the effect of the scanning strategy has been more often investigated on dentate arches,[15] the authors are only aware of in vitro studies for edentulous arches.[16]

Different strategies and techniques for scanning edentulous arches have been described,[6,7,17,18] but accuracy analyses are lacking. The authors are unaware of a definitive consensus in regard to the most suitable scanning strategy, but most intraoral scanner manufacturers recommend, at times without adequate evidence, a specific scanning strategy for their system.

Intraoral scanning of the edentulous mandible has been rarely investigated.[5,6,19] In a clinical setting, intraoral scanning of the edentulous mandible may be hindered by the presence of mobile mucosa and flabby tissues, while the cheeks and tongue may cover, at least in part, the residual ridge and hinder adequate accessibility of the scanner tip. Adequate displacement and stabilization of the mandibular soft tissues would generally require excessive stretching of the cheeks and pushing of the tongue, uncomfortable for the patient, reducing patient cooperation, and leading to unwanted patient movements. Therefore, a 2-step scanning strategy has been recommended by manufacturers for the edentulous mandible. The 2-step procedure requires scanning one side first and then moving to the other side, in conjunction with the use of specific instruments for the proper displacement and stabilization of the soft tissues. However, moving the scanner from one side to the other, with the potential tissue displacement and instability at the boundary of the 2 scanning fields, may hinder the stitching process, complicate the scanning procedure, and distort the resulting scan.

To provide data useful to address these issues, the 3-dimensional (3D) differences between the intraoral scans of edentulous mandibles made with a 2-step scanning strategy and conventional elastomeric impressions, as well as their potential distortion, were investigated in this clinical study. The null hypotheses were that no distortion would be found in intraoral scans of edentulous mandibular arches made with a 2-step scanning strategy and no difference in distortion would be found between intraoral scans and elastomeric impressions.

MATERIAL AND METHODS

The review board of the principal investigator's institution approved the study (approval number: 47/CE/2019). Twenty consecutive edentulous patients requiring complete mandibular dentures were included. All participants provided informed consent to be enrolled in the study. The edentulous mandibular arch (Fig. 1) was scanned by a single operator (L.L.R.) using an intraoral scanner (TRIOS 4; 3Shape A/S) and following the 2-step scanning strategy, directly accessible from the help function of the intraoral scanner

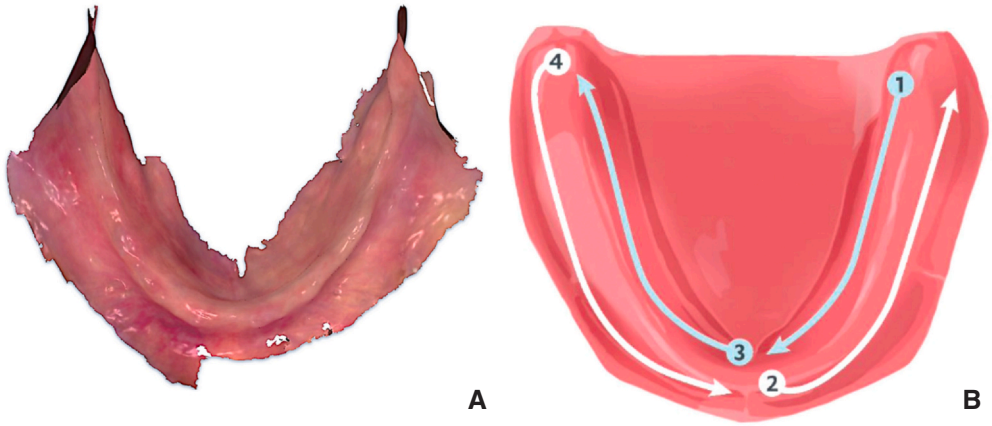

Figure 1. A, Intraoral scan of edentulous mandibular arch. B, Scanning strategy used for intraoral scanning.

software program (Fig.1B). A dedicated retractor system (Lo Russo Retractors; ELDO s.r.l.) was used to displace and stabilize the soft tissues (Fig. 2). The scans were imported into a software program (Dental System; 3Shape A/S) and used to design custom trays. The space for the impression material was set at 1.5 mm.[20] The trays were built by using a 3D printer (Prusa i3 MK3S; Prusa Research) and used to make a conventional impression with a polysulfide impression material (Permlastic; Kerr Corp) by following the manufacturer's instructions. The elastomeric impression was immediately scanned with the same intraoral scanner by the same investigator (Fig. 3). A direct scan of the elastomeric impression was chosen because the absence of voids and undercuts in edentulous arches was expected to minimize the shadowing effect.[21]

For every participant, the intraoral scan (S) and the scan of the elastomeric impression (C) were exported to the standard tessellation language (STL) format by using the intraoral scanner's software program. STL files were imported into a surface-matching software program

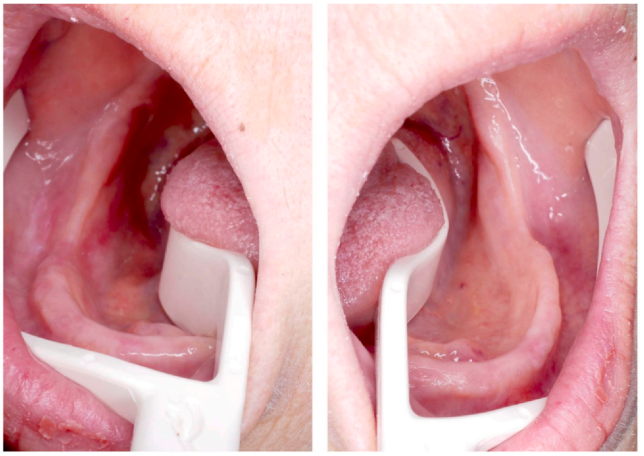

Figure 2. Dedicated retractor system (Lo Russo Retractors; ELDO s.r.l.) used to provide soft tissue retraction and stabilization. Left and right side.

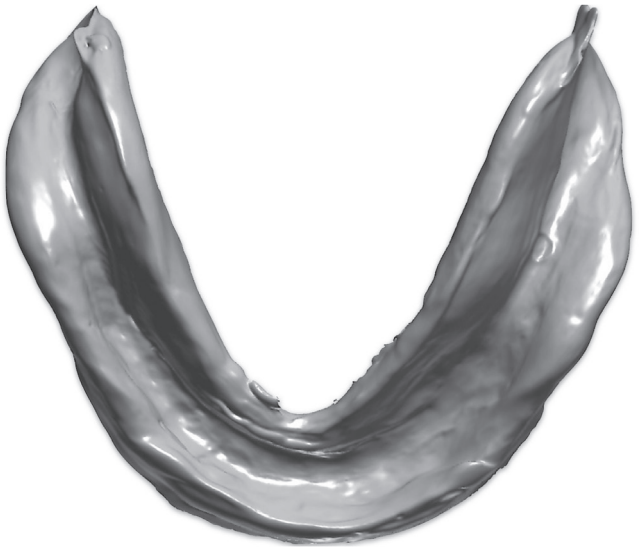

Figure 3. Scan of conventional impression in Figure 1A.

(Geomagic Wrap 2021; 3D Systems Inc), where a 2-phase best-fit alignment[5] was performed assuming S as reference and C as test object. Once aligned, S and C were made congruent by trimming peripheral areas which might have impaired both the alignment and the subsequent measurement accuracy.[5] This was done because the S captured zones would not be denture load bearing areas; as a result, the S was overextended as compared with C. To make them congruent, a curve was traced on C and used to trim and eliminate peripheral areas not present in either C or S (Fig. 4A). The curve was automatically projected onto S and used for trimming. As the trimmed S and C had comparable extension (Fig. 4B), a new best-fit alignment was performed to remove the potential alignment error caused by prior nonmatching areas. The position of the trimmed S and C in the global coordinate system was changed to ensure that any deviation between them were measured for deviations in the occlusal direction along the Z-axis,

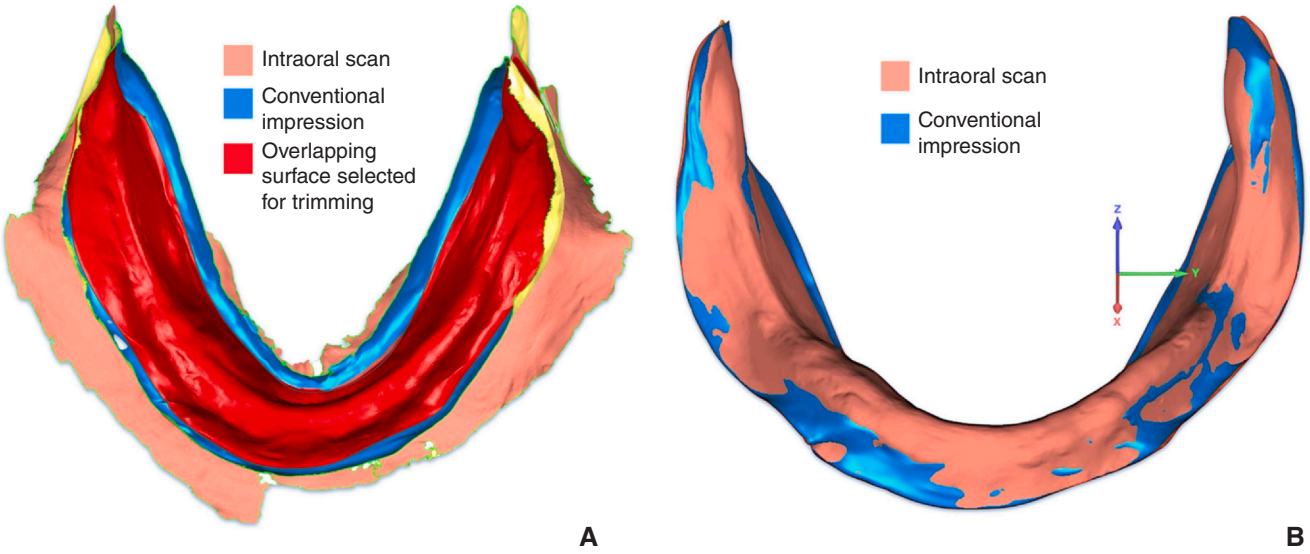

Figure 4. A, Superimposition and trimming of intraoral scan and conventional impression. B, Trimmed scans reoriented.

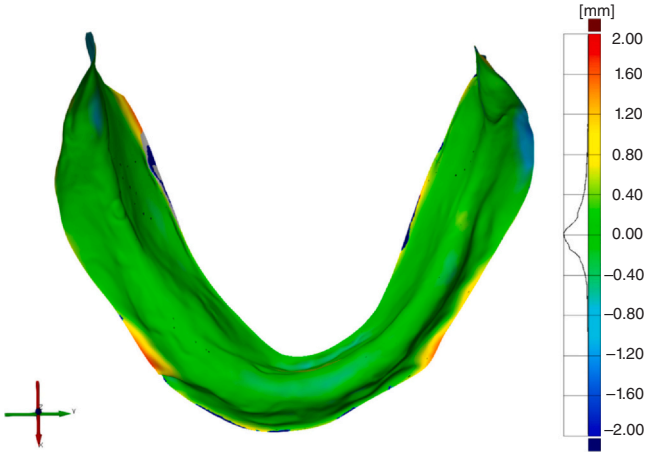

Figure 5. Color deviation map between intraoral scan and conventional impression of mandibular arch.

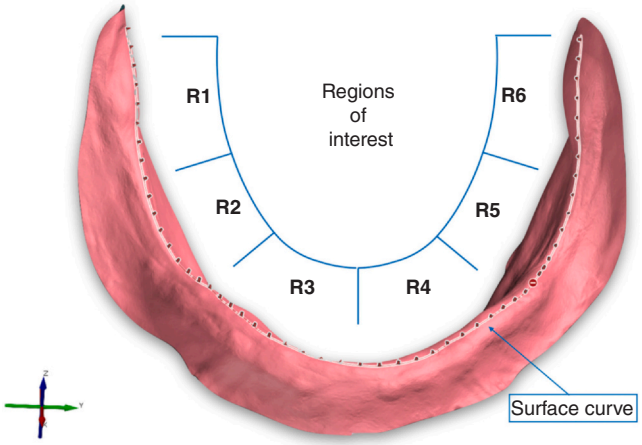

Figure 6. Surface curve traced on top of residual ridge of intraoral scan; visual representation of regions of interest along curve.

deviations in the sagittal plane along the X-axis, and deviations in the frontal plane along the Y-axis (Fig. 4B).

The trimmed and reoriented STLs of S and C were moved to a metrology software program (GOM Inspect Pro; Carl Zeiss GOM Metrology GmbH) for further comparison and analysis, assuming S as the reference scan. The mean 3D distance between S and C was measured and recorded as an indicator of the overall difference; a color difference map was also obtained for visualization (Fig. 5). A surface curve (SIOS) was traced on S, from the right to left retromolar pad, along the residual ridge crest (Fig. 6). SIOS was automatically projected onto C and a new curve (SC) was obtained. The mean distance between the SIOS and SC was measured and recorded as an indicator of the distortion under the assumption that, if the SIOS and SC were perfectly coincident and no distortion occurred, the SIOS would coincide with the SC and their relative distance would be zero. The overall distance between curves and their deviations along the X-, Y-, and Z-axes were recorded, corresponding (from the preliminary reorientation) to anteroposterior, mediolateral, and corono-apical deviation, respectively. Data regarding such deviations were automatically obtained and exported for further analysis. The corresponding dataset included, on average, 45 measurements per millimeter, made automatically by the software program along the SIOS and SC curves. Starting from the midline, the residual ridge and the corresponding curves were divided bilaterally into 3 regions of interest. This identified 3 segments of interest on each side: anterior, corresponding to the third closest to the midline; posterior, corresponding to the most distal third of the curve; and lateral, corresponding to the third between the anterior and posterior regions. The X-, Y-, and Z-axes deviations were therefore obtained for 6 regions of interest (R1: posterior-

Table 1. Statistical significance of differences between intraoral scans and conventional impressions

	Mean	SE	*P*
Full scans deviation (mm)	-0.08	0.025	**.003**[a]
Surface curves deviations			
X-axis deviation (mm) (Anteroposterior)	-0.02	0.004	**<.001**[b]
Y-axis deviation (mm) (Mediolateral)	-0.007	0.004	.069[b]
Z-axis deviation (mm) (Corono-apical)	-0.7	0.006	**<.001**[b]

SE, Standard error. **Bold** indicates statically significant differences ($P<.05$).

[a] One-sample *t* test; null hypothesis: mean distance between IOS and C zero.

[b] One-sample *t* test; null hypothesis: mean distance between SIOS and SC zero.

right; R2: lateral-right; R3: anterior-right; R4: anterior-left; R5: lateral-left; R6: posterior-left) (Fig. 6).

The 1-sample *t* test was used to investigate whether the overall difference between the S and C was significantly different from zero. The same was carried out to assess the significance of the mean X-, Y-, and Z-axis deviations by testing the following hypothesis: If the intraoral scan of the edentulous arch and the corresponding scan of the elastomeric impression were perfectly coincident and no deviations occurred, the distance between them at the measurement points along the curves traced on the residual ridge would be zero provided that an accurate superimposition was obtained. Hence, for data related to each axis, the 1-sample *t* test was used to answer the following question: Is the observed mean distance significantly different from zero? The effects of measurement positions between and within patients on discrepancies along the X-, Y-, and Z-axes were also investigated by using generalized estimated equation (GEE) models. The GEE methodology was used to model and control the within-unit measurements from the 6 regions of interest. The case was used as a subject-variable; side (right/left) and regions of interest were included as factors to investigate differences measured along each axis, while the variations of the remaining 2 axes were included as covariates. The statistical analyses were performed with a statistical software program (IBM SPSS Statistics, v25.0; IBM Corp) (α=.05).

RESULTS

The mean (−0.08 mm; standard error (SE): 0.025) distance between the S and C was significantly different from zero (P=.003) (Table 1). The minus sign indicated that the conventional impression was in a more apical position than in the intraoral scan. The mean deviations between SIOS and SC along the X- (−0.02 mm; SE: 0.004) (Fig. 7), Y- (−0.007 mm; SE: 0.004) (Fig. 8), and

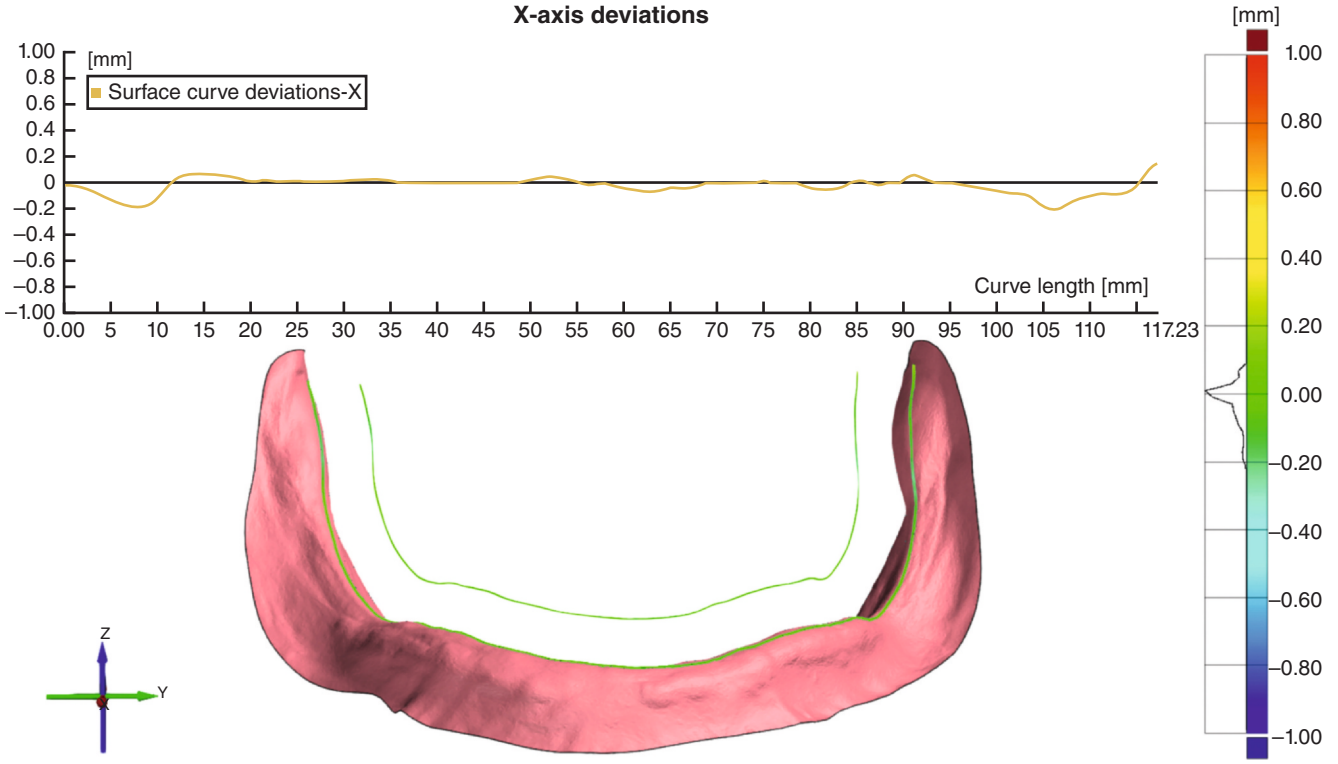

Figure 7. X-axis deviation measurements between surface curves. Diagram (top) and color deviation map (right).

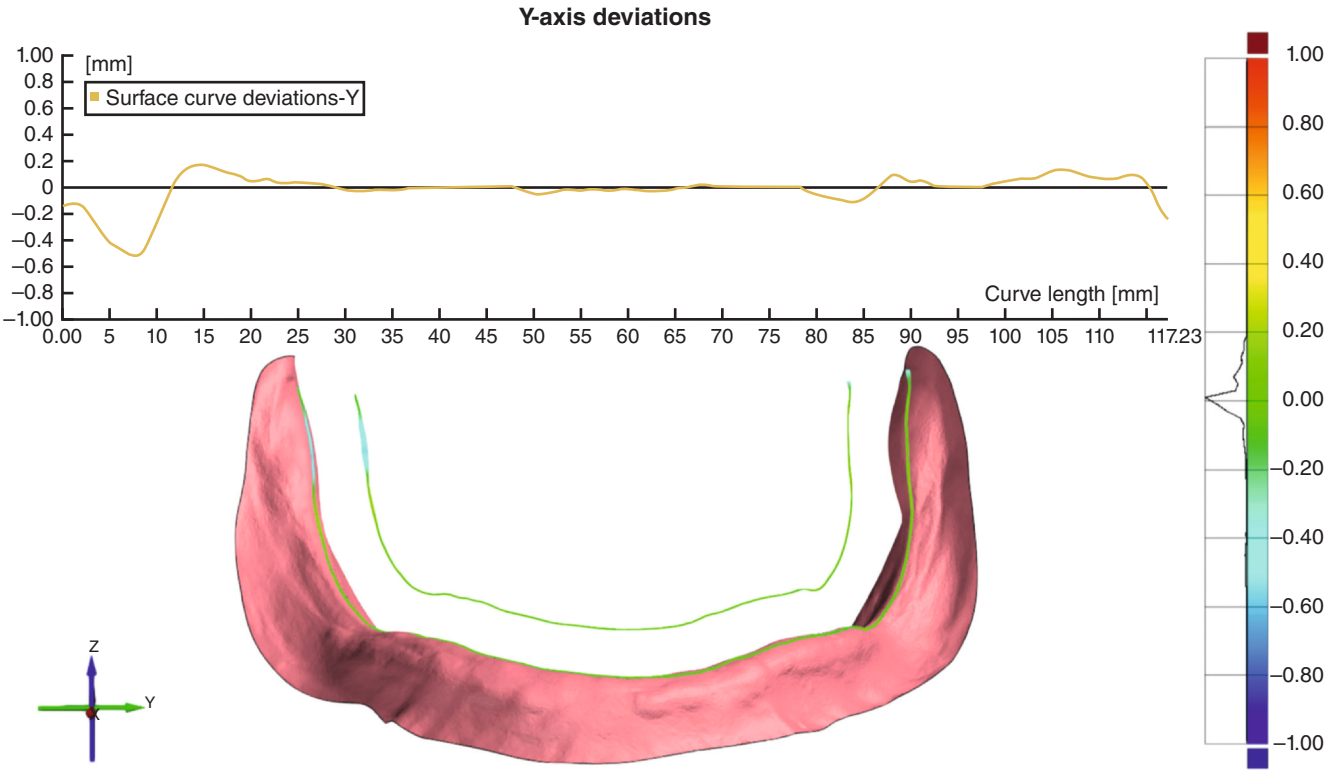

Figure 8. Y-axis deviation measurements between surface curves. Diagram (top) and color deviation map (right).

Z-axis (–0.7 mm; SE: 0.006 mm) (Fig. 9) were significantly different from zero for the X- and Z-axis ($P<.001$) but not for the Y-axis ($P=.069$). The GEE models addressing deviations between the SIOS and SC along the X-, Y-, and Z-axes, as well as their global 3D deviations, showed no significant effect of the factor "side" (Table 2), whereas a significant effect was found for the factor "region." Estimated marginal means for the X-, Y-, Z-axes and for the overall 3D (XYZ) deviations across the side and regions of interest are presented in Table 3. To address such deviations across regions of interest precisely, a pairwise comparison of mean differences as resulting from the GEE models with the Bonferroni adjustment for multiple comparisons was performed and is reported in Table 4.

DISCUSSION

Most of the studies regarding the accuracy of the intraoral scans of edentulous arches have been made in vitro and have generally addressed the maxillary arch.[7] Data gathered from clinical studies are scarce,[4,5] and the mandibular arch has seldom been investigated.[5,6,19] The precise measurement of the accuracy of intraoral scans has been reported to be problematic from a methodological standpoint and would ideally require a direct comparison of intraoral scans with the intraoral anatomy of the edentulous arches.[5] This was clearly not feasible, and, therefore, the only possible comparison was between intraoral scans and conventional impressions of the edentulous arches. Because both types of recording are ultimately replicas (digital or analog) of the anatomy of the edentulous arches, differences can be measured, but, based on such a measurement, none of them can be assumed as the standard and used as a reference to measure trueness of the other type of impression. Indeed, even a mucostatic conventional impression would exert some pressure on the oral mucosa and cause minor soft tissue displacement. As a result, it is not surprising that a difference exists between an intraoral scan of an edentulous arch and the corresponding conventional impression. Such a difference, as measured in the present clinical study, however, had a mean value of –0.08 mm, with the coordinates of the elastomeric impression located in a more apical position, likely because of the compression applied by the impression material.[5] The apical position was further confirmed by the analysis of curve deviations made on each reference axis. Indeed, the Z-axis, corresponding to pressure in the corono-apical direction during conventional impression making, showed the greatest deviation (–0.7 mm, on average), which was 35- to 100-fold greater than the deviations measured for the X- (–0.02 mm) and Y-axis (–0.007 mm), respectively. While a difference was found between the coordinates of the elastomeric impressions

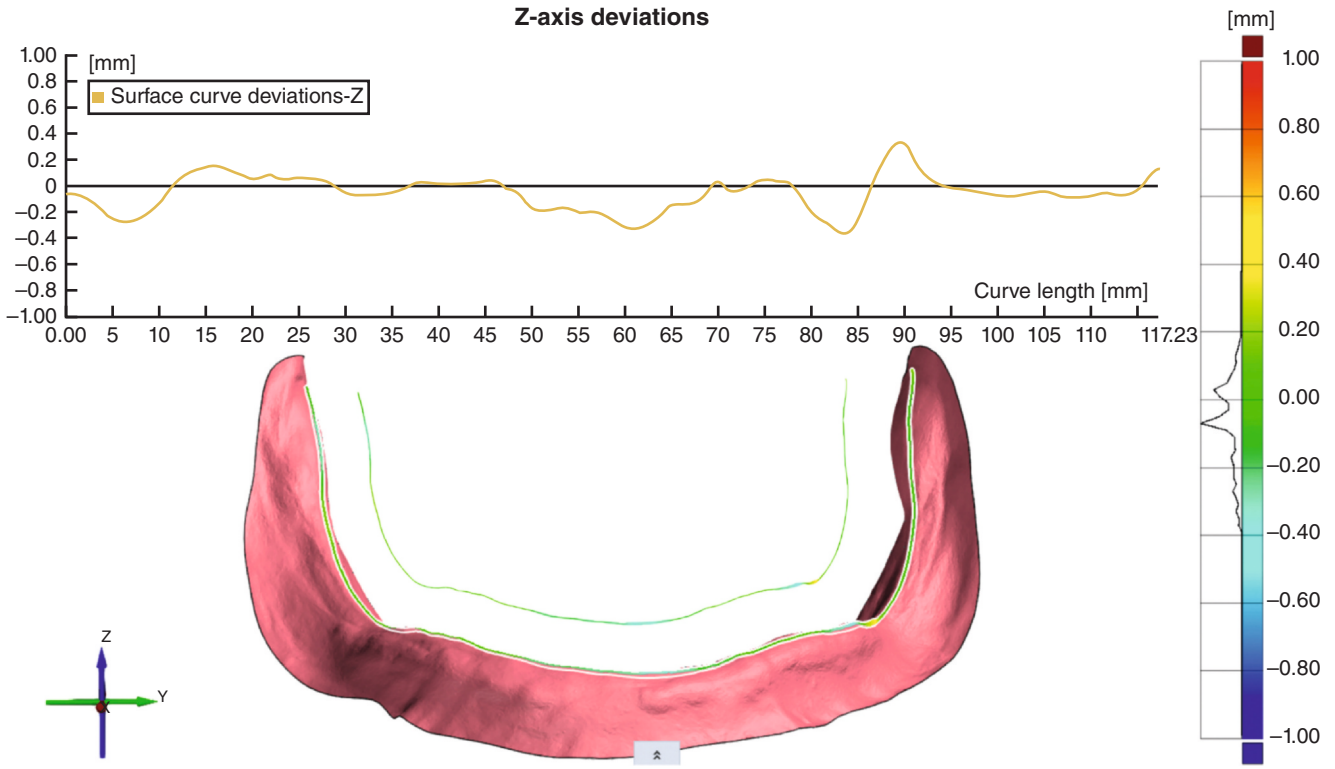

Figure 9. Z-axis deviation measurements between surface curves. Diagram (top) and color deviation map (below).

Table 2. Statistical significance of effects of investigated factors on scans deviation: results from generalized estimated equation models

Deviations Along Ridge Surface Curves	Side	Region
	P	*P*
X-axis (anteroposterior)	.716	**.014**
Y-axis (mediolateral)	.189	.477
Z-axis (corono-apical)	.597	.230
XYZ (3-dimensional)	.642	**.004**

Bold indicates statically significant differences ($P<.05$).

and intraoral scans, the clinical significance of this difference appears limited.

For the edentulous mandibular arch, because of practical clinical aspects of the scanning procedure (retraction of the tongue and cheek to improve scanner accessibility to the scanning field and stabilization of tissues surrounding the residual ridge), the intraoral scan should be captured in 2 steps. Merging the scans of the 2 sides at the midline might, in theory, cause some distortions (for example bending) leading to alterations in shape of the arch or loss of accuracy. Such a potential distortion of the intraoral scans of edentulous arches because of the 2-step scanning strategy was investigated in the present study, and the null hypothesis that no distortion would be found in intraoral scans of edentulous mandibular arches made with a 2-step scanning strategy and that no difference in distortion would be

Table 3. Estimated marginal means for X-, Y-, Z-axis and XYZ deviations across side and regions of interest

Investigated Factor	Deviations Along Ridge Surface Curves (mm)							
	X-axis Deviation (Anteroposterior)		Y-axis Deviation (Mediolateral)		Z-axis Deviation (Corono-apical)		XYZ Deviation (3-dimensional)	
	Mean	SE	Mean	SE	Mean	SE	Mean	SE
Side								
Right side	-0.030	0.021	-0.021	0.022	-0.065	0.031	0.245	0.037
Left side	-0.021	0.012	0.005	0.007	-0.082	0.024	0.227	0.029
Region								
R1 (Posterior-right)	-0.086	0.056	-0.068	0.056	-0.061	0.059	0.284	0.089
R2 (Lateral-right)	-0.011	0.016	0.005	0.017	-0.085	0.051	0.225	0.052
R3 (Anterior-right)	0.015	0.011	0.004	0.006	-0.046	0.034	0.221	0.038
R4 (Anterior-left)	0.007	0.011	0.009	0.010	-0.086	0.031	0.209	0.032
R5 (Lateral-left)	-0.006	0.007	-0.060	0.031	0.001	0.013	0.180	0.023
R6 (Posterior-left)	-0.067	0.041	0.006	0.023	-0.102	0.060	0.294	0.076

SE, Standard error.

Table 4. Pairwise comparisons across regions from generalized estimated equation models: mean differences and corresponding statistical significance with Bonferroni adjustment for multiple comparisons

Deviations Along Ridge Surface Curves												
Pairwise Comparison		X-axis Deviation (Anteroposterior)			Y-axis Deviation (Mediolateral)			Z-axis Deviation (Corono-apical)			XYZ Deviation (3-dimensional)		
Region (a)	Region (b)	Mean Difference (a-b)	SE	*P*	Mean Difference (a-b)	SE	*P*	Mean Difference (a-b)	SE	*P*	Mean Difference (a-b)	SE	*P*
R1	R2	-0.075	0.055	>.999	-0.072	0.051	>.999	0.023	0.071	>.999	0.059	0.101	>.999
	R3	-0.101	0.058	>.999	-0.072	0.059	>.999	-0.015	0.067	>.999	0.063	0.107	>.999
	R4	-0.094	0.057	>.999	-0.077	0.057	>.999	0.024	0.069	>.999	0.075	0.103	>.999
	R5	-0.080	0.054	>.999	-0.069	0.059	>.999	-0.001	0.062	>.999	0.104	0.093	>.999
	R6	-0.019	0.073	>.999	-0.073	0.050	>.999	0.041	0.092	>.999	-0.010	0.121	>.999
R2	R3	-0.026	0.022	>.999	0.000	0.016	>.999	-0.039	0.067	>.999	0.004	0.058	>.999
	R4	-0.018	0.019	>.999	-0.004	0.018	>.999	0.001	0.070	>.999	0.016	0.065	>.999
	R5	-0.005	0.014	>.999	0.004	0.028	>.999	-0.025	0.037	>.999	0.045	0.039	>.999
	R6	0.056	0.050	>.999	-0.001	0.019	>.999	0.017	0.056	>.999	-0.069	0.064	>.999
R3	R4	0.007	0.015	>.999	-0.005	0.011	>.999	0.039	0.046	>.999	0.012	0.031	>.999
	R5	0.021	0.013	>.999	0.003	0.017	>.999	0.014	0.050	>.999	0.041	0.039	>.999
	R6	0.081	0.038	.513	-0.001	0.023	>.999	0.056	0.058	>.999	-0.073	0.075	>.999
R4	R5	0.013	0.012	>.999	0.008	0.016	>.999	-0.026	0.049	>.999	0.030	0.039	>.999
	R6	0.074	0.045	>.999	0.003	0.026	>.999	0.016	0.080	>.999	-0.085	0.093	>.999
R5	R6	0.061	0.046	>.999	-0.005	0.032	>.999	0.042	0.050	>.999	-0.114	0.064	>.999

SE, Standard error.

found between intraoral scans and elastomeric impressions was not rejected.

The results confirmed that the mean full scan deviation was minimal (–0.08 mm), with no evident deviation pattern in the color map evaluation (Fig. 5). The mean differences between the right and left side were 0.009 mm, 0.025 mm, 0.017 mm, and 0.018 mm for the X- (anteroposterior), Y- (mediolateral), Z-axis (corono-apical), and overall 3D deviation, respectively (Table 3), which, related to the fabrication of removable prostheses, appear clinically not relevant.

In the presence of difference, if a distortion had occurred, it seems reasonable to expect lack of consistency of such a difference between sides or among regions. On this basis, the GEE models were used to assess the effects of side and region on deviations measured all along the surface curves, considering the X-, Y-, Z-axes and the overall 3D deviation, under the assumption that a distortion can be defined as a nonuniform or nonconsistent difference between sides or across regions. Results from the GEE models showed that deviations were consistent throughout the arch on the right and left side, with no significant effect found for the side in any of the 3D global deviation or X-, Y-, and Z-axis deviations (Table 2). Conversely, a significant effect was found for the region factor only in 3D global deviation (P=.004) and in X-axis deviation (P=.014). If such a significant effect of region accounts for an actual distortion, it would be reasonable to expect significant differences between corresponding regions (posterior regions=R1, R6; lateral regions=R2, R5; anterior regions=R3, R4;) on the 2 sides: this was not confirmed by the region pairwise comparisons (Table 4) of estimated marginal means from the GEE models after Bonferroni adjustment for multiple comparisons, which showed no statistical significance (P>.05).

Current results are applicable to the present experimental settings and reported technology or system, scanning strategy, and scanning auxiliary instruments. Future research should address such potential limitations in the context of different systems or clinical procedures.

CONCLUSIONS

Based on the findings of this clinical study, the following conclusions were drawn:

1. Intraoral scans of the edentulous mandibular arch made with a 2-step scanning strategy do not exhibit significant distortion in comparison with conventional elastomeric impressions.
2. Adequate management of the stability of tissues around the residual ridge, favoring accessibility for the scanner, can yield reliable intraoral scans of the edentulous mandibular arch.

PATIENT CONSENT

Informed patient consent has been obtained.

REFERENCES

1. Lo Russo L, Salamini A. Single-arch digital removable complete denture: A workflow that starts from the intraoral scan. *J Prosthet Dent*. 2018;120:20–24.
2. Lo Russo L, Salamini A, Troiano G, Guida L. Digital dentures: A protocol based on intraoral scans. *J Prosthet Dent*. 2021;125:597–602.
3. Lo Russo L, Zhurakivska K, Guida L, Chochlidakis K, Troiano G, Ercoli C. Comparative cost-analysis for removable complete dentures fabricated with conventional, partial, and complete digital workflows. *J Prosthet Dent* 2022.
4. Chebib N, Kalberer N, Srinivasan M, Maniewicz S, Perneger T, Müller F. Edentulous jaw impression techniques: An in vivo comparison of trueness. *J Prosthet Dent*. 2019;121:623–630.
5. Lo Russo L, Caradonna G, Troiano G, Salamini A, Guida L, Ciavarella D. Three-dimensional differences between intraoral scans and conventional impressions of edentulous jaws: A clinical study. *J Prosthet Dent*. 2020;123:264–268.
6. Hack G, Liberman L, Vach K, Tchorz JP, Kohal RJ, Patzelt SBM. Computerized optical impression making of edentulous jaws - An in vivo feasibility study. *J Prosthodont Res*. 2020;64:444–453.
7. Zarone F, Ruggiero G, Ferrari M, Mangano F, Joda T, Sorrentino R. Comparison of different intraoral scanning techniques on the completely edentulous maxilla: An in vitro 3-dimensional comparative analysis. *J Prosthet Dent*. 2020;124(762). e1-8.
8. Rasaie V, Abduo J, Hashemi S. Accuracy of intraoral scanners for recording the denture bearing areas: A systematic review. *J Prosthodont*. 2021;30:520–539.
9. Kim JE, Amelya A, Shin Y, Shim JS. Accuracy of intraoral digital impressions using an artificial landmark. *J Prosthet Dent*. 2017;117:755–761.
10. Waldecker M, Rues S, Awounvo Awounvo JS, Rammelsberg P, Bömicke W. In vitro accuracy of digital and conventional impressions in the partially edentulous maxilla. *Clin Oral Investig*. 2022;26:6491–6502.
11. Fang JH, An X, Jeong SM, Choi BH. Digital intraoral scanning technique for edentulous jaws. *J Prosthet Dent*. 2018;119:733–735.
12. Ciano J, Beatty BL. Regional quantitative histological variations in human oral mucosa. *Anat Rec*. 2015;298:562–578.
13. Chebib N, Imamura Y, El Osta N, Srinivasan M, Müller F, Maniewicz S. Fit and retention of complete denture bases: Part II - conventional impressions versus digital scans: A clinical controlled crossover study. *J Prosthet Dent* 2022.
14. Xie Q, Närhi TO, Nevalainen JM, Wolf J, Ainamo A. Oral status and prosthetic factors related to residual ridge resorption in elderly subjects. *Acta Odontol Scand*. 1997;55:306–313.
15. Latham J, Ludlow M, Mennito A, Kelly A, Evans Z, Renne W. Effect of scan pattern on complete-arch scans with 4 digital scanners. *J Prosthet Dent*. 2020;123:85–95.
16. Jamjoom FZ, Aldghim A, Aldibasi O, Yilmaz B. Impact of intraoral scanner, scanning strategy, and scanned arch on the scan accuracy of edentulous arches: An in vitro study. *J Prosthet Dent* 2023.
17. Li J, Moon HS, Kim JH, Yoon HI, Oh KC. Accuracy of impression-making methods in edentulous arches: An in vitro study encompassing conventional and digital methods. *J Prosthet Dent*. 2022;128:479–486.
18. Jung S, Park C, Yang HS, et al. Comparison of different impression techniques for edentulous jaws using three-dimensional analysis. *J Adv Prosthodont*. 2019;11:179–186.
19. Al Hamad KQ, Al-Kaff FT. Trueness of intraoral scanning of edentulous arches: A comparative clinical study. *J Prosthodont*. 2023;32:26–31.
20. Razek MK. Assessment of tissue conditioning materials for functional impressions. *J Prosthet Dent*. 1979;42:376–380.
21. Quaas S, Rudolph H, Luthardt RG. Direct mechanical data acquisition of dental impressions for the manufacturing of CAD/CAM restorations. *J Dent*. 2007;35:903–908.

Corresponding author:
Prof Lucio Lo Russo
Department of Clinical and Experimental Medicine
School of Dentistry
University of Foggia
Via Serro D'Annunzio, 20
Vallesaccarda, Avellino 83050
ITALY
Email: lucio.lorusso@unifg.it.

https://doi.org/10.1016/j.prosdent.2023.09.029